Enhanced Knowledge in Sciences and Technology Vol. 2 No. 2 (2022) 309-317

EKST

Homepage: http://publisher.uthm.edu.my/periodicals/index.php/ekst
e-ISSN: 2773-6385

Characterization of ITO as a Top Layer for Solar Cell Application

Nur Qutren Nada Khyrun Anuar[1], **Ahmad Hadi Ali**[2] *

[1 2] Photonics Devices and Sensor Research Center (PDSR),
Department of Physics and Chemistry,
Faculty of Applied Sciences and Technology, Pagoh Educational Hub,
Universiti Tun Hussein Onn Malaysia,
84600, Pagoh, Johor, MALAYSIA

*Corresponding Author Designation

DOI: https://doi.org/10.30880/ekst.2022.02.02.033
Received 02 January 2022; Accepted 02 March 2022; Available online 23 November 2022

Abstract: In solar cells application, ITO thin films can be used as a top layer which can act as a contact layer, current spreading layer and window layer. ITO has a high transparency in the visible range, good electrical conductivity, and wide bandgap energy. However, P-type silicon (Si) that used in solar cell structure causes high reflection of light on the surface which will lower the resistivity of solar cells. Besides, layer of ITO films added on top of Si causes a potential barrier created between them. In this study, a different thicknesses of ITO was deposited onto the Si and glass substrates. The samples were characterised based on the optical, electrical, and topological characteristics. From UV-Vis spectrometer, transmittance graphs show decreasing trends with increasing thickness, while absorbance graph shows opposite trends. From four-point probe, the resistivity has also found to be decreasing exponentially with various thicknesses. The AFM results show an increment of the grain size and exponent increment of RMS roughness along with the thickness. Finally, figure of merit is used to compare the optical transmittance and sheet resistance between ITO films. From that, the optimum thickness of 400 nm ITO film with the best properties is obtained.

Keywords: ITO, Solar Cells, UV-Vis Spectrometer, Four-Point Probe, AFM

1. Introduction

Transparent conductive oxides (TCO) are known to be optically transparent and electrically conductive materials. TCOs conductivity can be adjusted from insulating through semiconducting to

**Corresponding author: ahadi@uthm.edu.my*

conducting the same as their transparency which can be changed[1] . Usually, TCOs thin films are used in many application including solar cells [2], liquid-crystal displays [3], and flat panel displays[3] . Some of TCO materials such as indium oxide (In_2O_3) can be doped to improve the electrical properties without degrading its optical properties. The most common TCO thin film that have been doped is tin-doped indium, ITO. ITO has a high transparency in the visible range, good electrical conductivity, and wide bandgap energy. ITO thin films have been widely investigated on substrates such as glass and silicon to understand more about its properties.

Most of solar cells application used P-type silicon (Si) in the solar cell structure. However, material Si has high refractive index, n which is 3.42-3.48 [4]. This causes a high reflection of light on the surface of Si. When the layer of ITO is added on top of Si, it can minimize the reflection of light and increase resistivity of solar cells. This is because ITO has lower refractive index compared to Si. Besides, the mismatch of ITO and Si causes a contact resistance because of a potential barrier created between them. This barrier creates electric field that provides force. This force slows down the movement of electrons. To overcome this barrier, electrons need more energy to flow over from ITO to Si.

Therefore, ITO as a top layer of solar cell applications can act as a contact layer, current spreading layer and window layer. Different thicknesses of ITO thin films will give different properties as it will affects the performances of solar cell application. The studies about the effect of ITO thin film thickness have been observed by other researchers [5],[6],[7]. ITO-Si contact has been used in solar cells. Basically, this contact layer is used to conduct electrical current to load to be stored for future utility. Moreover, ITO can be used as current spreading layers in order to decrease contact resistance and enhance carrier distribution. ITO thin film will be used to ease current conduction in the solar cells. The ITO performance is found to be more affected by the absorbance properties of the contact layers than their contact resistances [8]. Other than that, ITO has a low refractive index and has good adhesion with Si. It can also be used as an antireflection coating for window layer by selecting an appropriate thickness.

Besides that, ITO is a great alternative to substitute metal with a n-type semiconductor and can be used as transparent conductive electrodes. The desired properties that are needed from ITO are high electrical conductivity and good optical transmission. This can allow potential barriers such as Schottky characteristics. Usually, a semiconductor such as Si is used as an active component in the Schottky diode. The differences in work functions of the electrode and the adjacent semiconductor layer determine the Schottky barrier properties at the electrode/semiconductor interface.

In this study, a different thicknesses of ITO thin films were deposited onto the Si and glass substrates. These samples were characterized based on optical, electrical and topological properties. From the analysis of characterization samples, the optimum thickness of ITO was determine based on the figure of merit. Figure of merit is important as it is use to investigate the dependency of ITO thin films thickness on the optical transmittance and sheet resistance. Using figure of merit, the performances for each thickness were compared based on optical transmittance and sheet resistance properties.

2. Materials and Methods

In this study, ITO thin film was deposited by DC sputtering system model Q150RS. By using two independent sputtering head sequentially with different deposition time, the ITO was sputtered onto the Si and glass substrates [6]. The films thicknesses were estimated using DC sputtering system without measuring the exact deposition time. The film nominal thicknesses are 100 nm, 200 nm, 300 nm, 400 nm, 500 nm and 600 nm. The sputtering current was set at 80 mA and the base pressure was pumped by the chamber between 5×10^3 mbar to 3×10^3 mbar. The Si substrates were cleaned with ultrasonic cleaner in acetone solution, isopropyl, distilled water, and N^2 blow before deposition. Meanwhile, the Decon-90 glass cleaner was used to clean the glass samples. Then, in a plasma cleaner, they were exposed to intense RF waves for 15 minutes.

The characterization of ITO thin film begin with UV/Vis-NIR spectrophotometer (UV-3699 Plus) SHIMADZU spectrometer to determine the optical properties of ITO thin film. The wavelength range used were 300-1500 nm. The electrical properties were analysed by using four-point probes [7]. Moreover, topological properties were studied by Bruker Dimension Edge atomic force microscope (AFM) to determine the grain size and the roughness of ITO thin film [9].

3. Results and Discussion

3.1 Optical Properties of ITO Thin Films

UV-Visible Spectrometry was used to identify the optical properties of ITO thin films. The optical properties are transmittance, absorbance, and bandgap. The optical transmittance of samples was measured in the wavelength range between 300 nm to 800 nm. From the optical transmittance spectra that were measured using UV-vis spectrometer, the graph of transmittance T (%) vs wavelength λ (nm) and graph of absorbance A (Au) vs wavelength λ (nm) were obtained. The graphs were constructed again in Origin lab software.

Figure 1 shows the Transmittance T (%) vs Wavelength λ (nm) graph for difference thicknesses of ITO for 100 nm, 200 nm, 300 nm, 400 nm, 500 nm, and 600 nm. From wavelength range of 300-800 nm, the transmittance graph seen to be independent with the ITO thicknesses in the visible region. ITO thin films have a properties of high transparency to the visible region. Therefore, the increase in transmittance with decrease in thicknesses of ITO thin films have been observed and also by other researcher[10]. The effect of grain size can be related to this phenomena. The grain size increases as the thin film thickness increases (see Figure 7), causing light scattering.

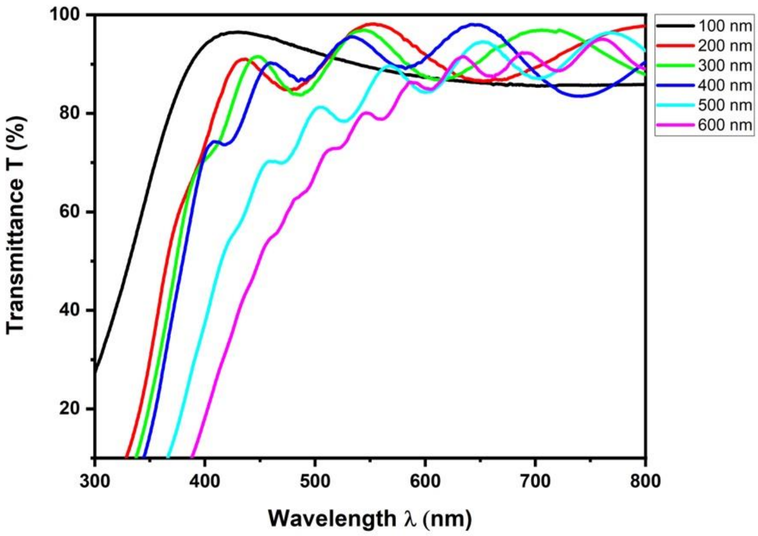

Figure 1: Graph of transmittance T (%) with wavelength λ (nm) for various thicknesses of ITO

The fluctuation on transmittance spectrum of ITO thin film thicknesses for 600 nm and 500 nm are observed. This phenomenon called interferences fringes in transmission of thin films. The similar observation has been observed by other researcher[4].

Figure 2 shows the plot of Absorbance A (Au) vs Wavelength λ (nm) graph for difference thicknesses of ITO thin films. The absorbance studies were carried out in the wavelength range of 300-800 nm. The absorbance spectra of ITO films show the opposite trend of transmittance spectra. With increasing thickness, free carrier absorption that increases carrier concentration in thick film and leads to the absorption of more light causes the average transmittance decreases slightly.

The energy gap values were determine and plotted from the Tauc relation, $(\alpha h\nu)^2 = h\upsilon - Eg$ [9]. Moreover, absorbances are related to the bandgap. This is because the tangent of linear part of the plot of $(\alpha h\nu)^2$ vs $h\nu$ (e.V) were used to calculate the values of bandgap for ITO thin films where α is the absorption coefficient. Absorption coefficient is used as a function of photon energy which can be expressed in Tauc relation. As shown in Table 1, the bandgap energy, E_g values obtained decreased from 3.58 eV to 3.14 eV with the increased thickness of ITO thin films. By increasing the thickness, the absorption coefficient increased and the band gap decreased. This studies also has been observed by other researchers [9],[11].

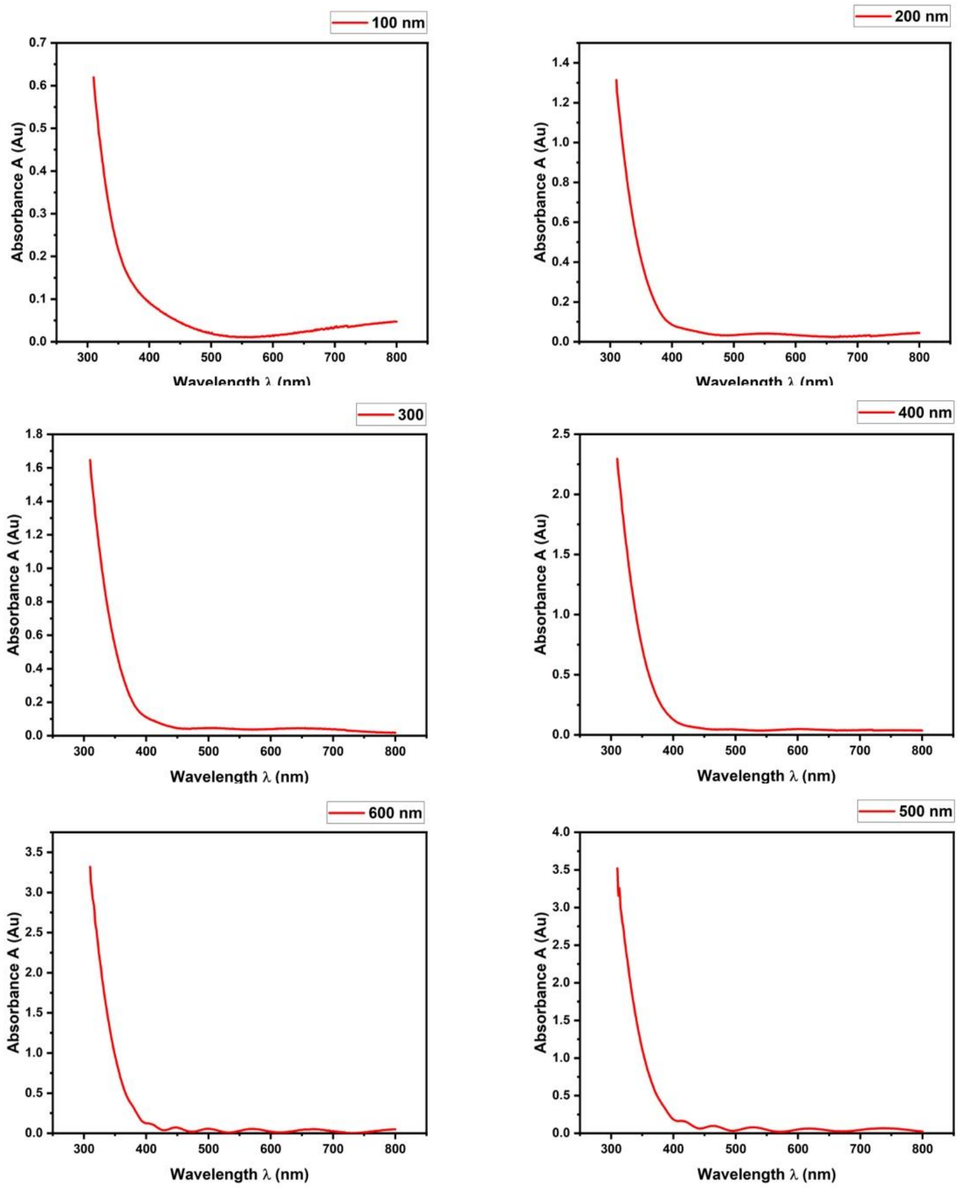

Figure 2: The plot of absorbance A (Au) with wavelength λ (nm) for various thicknesses of ITO thin films.

Table 1: Bandgap values, E_g of ITO thin films.

Thickness of ITO thin film (nm)	100	200	300	400	500	600
hv (eV)	3.58	3.50	3.31	3.28	3.24	3.14

3.2 Electrical Properties of ITO Thin Films

Four-point probe was used to identify the electrical properties of ITO thin films. In this method, the electrical resistivity of thin films of ITO were measured for different thickness of thin films of ITO. We obtained values of resistivity,ρ for this experiment. Figure 3 shows Resistivity $\rho \times 10^{-4}$ $(\Omega \cdot \mathrm{cm})$ vs thickness of ITO thin film (nm) graph. It is observed that the resistivity decreased with the increasing of ITO film thickness. This observation also had been observed by other researchers [12],[6]. Resistivity seen to be related to grain size properties (see Figure 7) . Different conductivity is mostly caused by grain boundary scattering. The charge carriers can be scattered by the grain boundary. As a result of increasing grain size while decreasing grain boundary, conductivity increased, resulting in decreased resistivity.

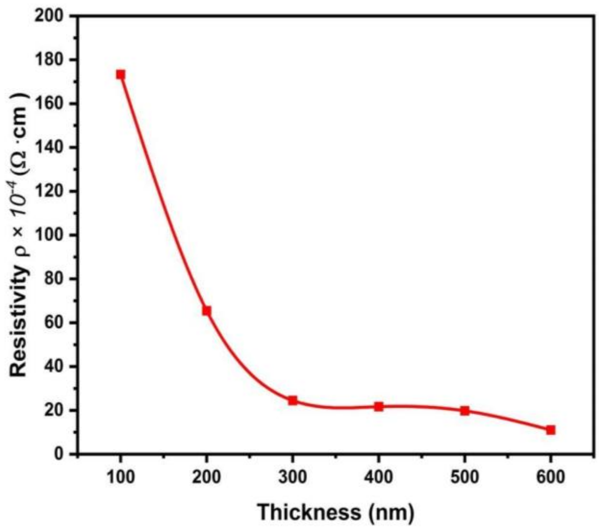

Figure 3: Resistivity $\boldsymbol{\rho \times 10^{-4}}$ $(\boldsymbol{\Omega \cdot \mathrm{cm}})$ obtained for different thicknesses of deposited ITO thin film (nm).

Figure of merit, F_H was used to compare the performance of ITO films using their electrical sheet resistance and optical transmission. The equation for figure of merit used was developed by Haacke [13].

$$F_H = \frac{T^{10}}{R_s}. \qquad Eq\ 1$$

where, T = optical transmittance and Rs = sheet resistance. Sheet resistance values were calculated by using an equation that was defined by[14] where, ρ = resistivity and t = thickness: $R_s = \frac{\rho}{t}$.

Because of its high transmittance and low sheet resistance, a thickness of 400 nm obtained is the highest figure of merit. In the meantime, a thickness of 100 nm yielded the lowest figure of merit. A high sheet resistance was responsible for this. These observations were also mentioned by [7].

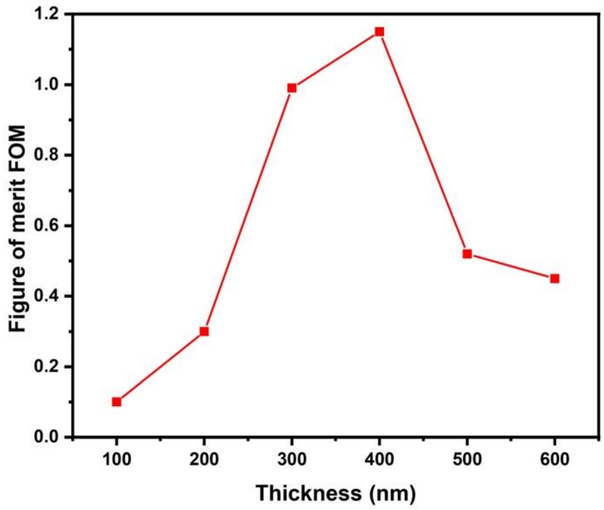

Figure 4: Values of Figure of merit, FOM for various thicknesses of ITO thin films (nm).

3.3 Topological Properties of ITO Thin Films

For topological properties of ITO thin films, we used AFM. We able to determine material properties from the AFM techniques such as RMS roughness and grain size. Figure 5 shows the 2D AFM images of ITO films with different thickness. ITO thin films surface show continuous island-like structures. When the thickness of thin films decreasing, the films exhibit tiny grain growth by some bigger grains. Therefore, the thin films have no uniform structure. However, by increasing the thickness of thin films, small grains combine which form bigger grains and a columnar structure is observed. The bigger grains provide for clusters and a dense and uniform structure. These observations had also been observed by other researchers [15].

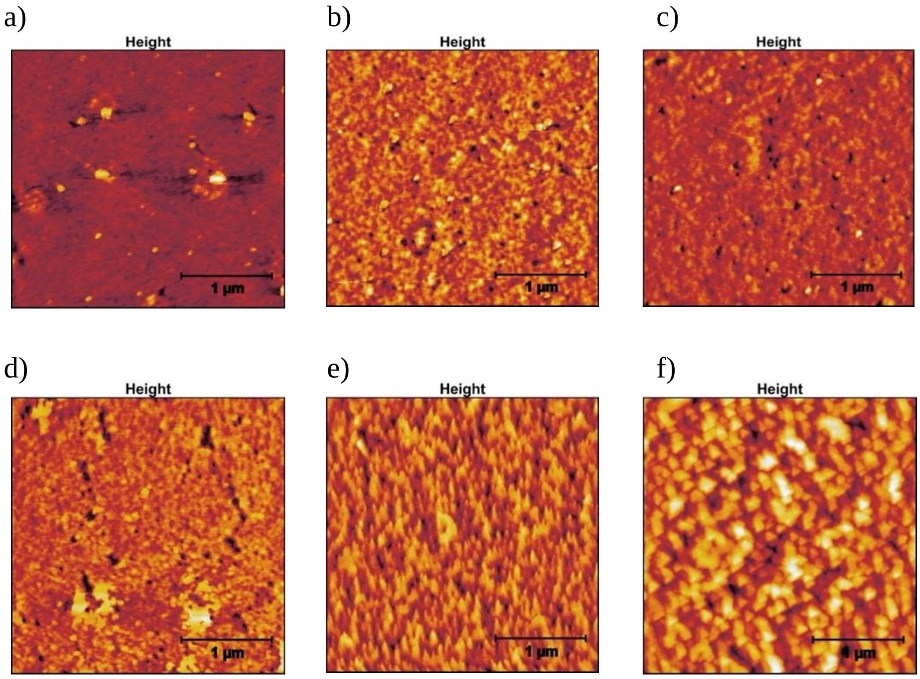

Figure 5: AFM 2D image of prepared ITO thin films of various thicknesses of ITO, a) 100 nm, b) 200 nm, c) 300 nm, d) 400 nm, e) 500 nm, f) 600 nm.

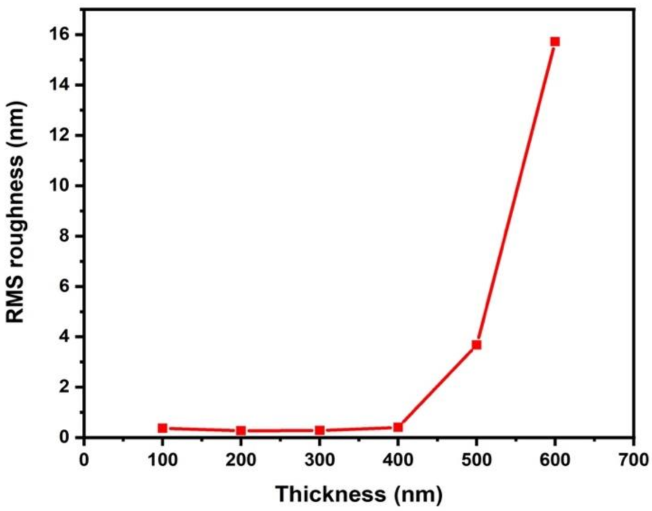

Figure 6: RMS roughness (nm) of various thicknesses of ITO thin films.

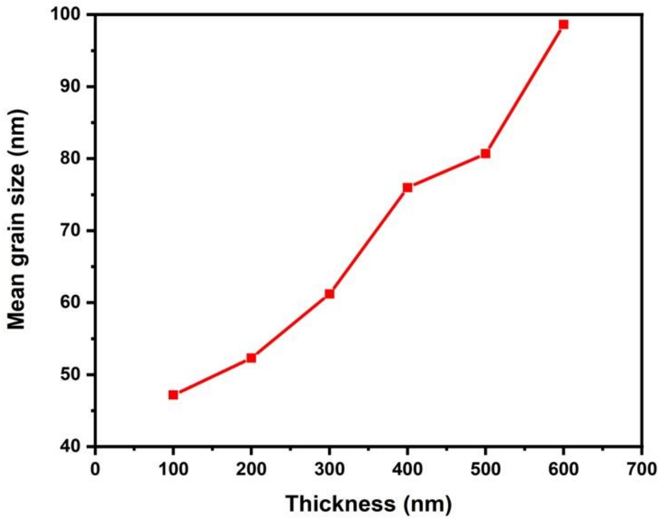

Figure 7: Mean grain size (nm) of various thicknesses of ITO thin films.

The relationship between RMS roughness and grain size with ITO films thickness are shown in Figure 6 and Figure 7 The RMS roughness of ITO films is exponentially increase with the thickness of ITO films. Same as the mean grain size of ITO films is increasing with the thickness of ITO films. When the thicknesses of ITO thin films increase, less impact of the roughness due to the substrate and more uniform structure of the ITO thin films. These observations had also been observed by other researchers [10], [15], [10]

4. Conclusion

In this study, the optical, electrical, and topological properties of ITO films were investigated as a function of the film thickness. For 400 nm film thickness, the transmittance value is 75 % and the bandgap energy value is 3.28 eV. Meanwhile, the resistivity value obtained from four-point probe for 400 nm is 21.7 $\Omega \cdot$ cm . Moreover, the topological properties were observed from AFM images. The RMS roughness and mean grain size of ITO thin film for 400 nm are 0.402 nm and 76 nm respectively. Finally, figure of merit, F_H was used to compare the performance of ITO films using their electrical sheet resistance and optical transmission. The highest figure of merit was obtained for a thickness of

400 nm due to its high transmittance and low sheet resistance. Therefore, from these analysis, it is found that the optimum thickness of ITO film is 400 nm with the values of 1.15 Ω^{-1}.

Acknowledgement

The author(s) would like to thank the Government of Malaysia and Universiti Tun Hussein Onn Malaysia for funding this research project through the UTHM TIER1 Grant (H845).

References

[1] A. Stadler. “Transparent Conducting Oxides - An Up-To-Date Overview,” Materials, vol. 5, no. 12, pp. 661–683. 2012.

[2] P. P. Horley, L. L. Jiménez, S. P. García, , J. Á. Quintana, Y. V. Vorobiev, R. R. Bon, and J. G. Hernández. “Thin Film Solar Cells: Modeling, obtaining and applications,” Application of Solar Energy, 95. 2013.

[3] S. K. Park, J. I., Han, W. K., Kim, and M. G. Kwak. “Deposition of indium tin oxide films on polymer substrates for application in plastic-based flat panel displays,” Thin Solid Films, 397(1-2), 49-55. 2001.

[4] M. Naser, A. Zaliman, S. Uda, H., and A. D. Yarub. “Investigation of the absorption coefficient, refractive index, energy band gap, and film thickness for Al0. 11Ga0. 89N, Al0. 03Ga0. 97N, and GaN by optical transmission method,” Int. J. Nanoelectronics and Materials 2 (2009) 189-195. 2009.

[5] M. D. Benoy, E. M. Mohammed, M. Suresh Babu, P. J. Binu, and B.Pradeep. “Thickness dependence of the properties of indium tin oxide (ITO) films prepared by activated reactive evaporation,” Brazilian Journal of Physics, 39, 629-632. 2009.

[6] H. Kim, J. S. Horwitz, G. Kushto, A. Pique, Z. H. Kafafi, C. M. Gilmore, & D. B. Chrisey. “Effect of film thickness on the properties of indium tin oxide thin films,” Journal of Applied Physics, 88(10), 6021-6025. 2000.

[7] M. Mazur, D. Kaczmarek, J. Domaradzki, D. Wojcieszak, S. Song, and F. Placido. “Influence of thickness on transparency and sheet resistance of ITO thin films,” Conference Proceedings - The 8th International Conference on Advanced Semiconductor Devices and Microsystems, ASDAM 2010, pp. 65–68. 2010.

[8] M. S. Points. “Optimization of ohmic contacts and current spreading layers for GaN based solar cells,” NNIN REU Research Accomplishments, 110-111. 2008.

[9] A. Hacini, A. H. Ali, and N. N. Adnan. “Optimization of ITO thin film properties as a function of deposition time using the swanepoel method,” Optical Materials, 120, 111411. 2021.

[10] S. H. Mohamed, F. M. El-Hossary, G. A. Gamal, and M. M. Kahlid. “Properties of indium tin oxide thin films deposited on polymer substrates,” Acta physica polonica A, 115(3), 704-708. 2009.

[11] M. Thirumoorthi and J. Thomas Joseph Prakash. “Structure, optical and electrical properties of indium tin oxide ultra-thin films prepared by jet nebulizer spray pyrolysis technique,” Journal of Asian Ceramic Societies, vol. 4, no. 1, pp. 124–132. 2016 .

[12] K. P. Sibin, N. Swain, P. Chowdhury, A. Dey, N. Sridhara, H. D. Shashikala, and H. C. Barshilia. “Optical and electrical properties of ITO thin films sputtered on flexible FEP substrate as passive thermal control system for space applications,” Solar Energy Materials and Solar Cells, 145, 314-322. 2016.

[13] S. A. Knickerbocker, and A. K. Kulkarni. “Calculation of the figure of merit for indium tin oxide films based on basic theory,” Journal of Vacuum Science & Technology A: Vacuum, Surfaces, and Films, 13(3), 1048-1052. 1995.

[14] M. Naftaly, S. Das, J. Gallop, K. Pan, F. Alkhalil, D. Kariyapperuma, and L. Hao. “Sheet resistance measurements of conductive thin films: A comparison of techniques,” Electronics, 10(8), 960. 2021.

[15] M. Z. H. Khan. “Pretreatment of ITO electrode and its physiochemical properties: Towards device fabrication,” Surface Engineering and Applied Electrochemistry, vol. 52, no. 6, pp. 547–564. 2016.